Available online at www.sciencedirect.com

SCIENCE DIRECT®

Tectonophysics 408 (2005) 101–112

TECTONOPHYSICS

www.elsevier.com/locate/tecto

High-resolution stratigraphy reveals repeated earthquake faulting in the Masada Fault Zone, Dead Sea Transform

Shmuel Marco [a,*], Amotz Agnon [b]

[a] *Department of Geophysics and Planetary Sciences, Tel Aviv University, Israel*
[b] *Institute of Earth Sciences, The Hebrew University, Jerusalem, Israel*

Received 1 October 2001; accepted 31 May 2005
Available online 19 September 2005

Abstract

A detailed study of the syndepositional Masada Fault Zone (MFZ) provides an example for fundamental characteristics of earthquakes, such as long term temporal clustering, repeated faulting on the same planes for a limited time of the order of a few thousands of years, and the formation of subaqueous breccia layers interpreted as seismites. The MFZ was studied in outcrops of 70–15 ka Lake Lisan sediments. Detailed columnar sections on both sides of well-exposed faults show that each individual fault exhibits a cluster, up to 4 ky long, with 3–5 slip events on the same plane. Each slip event is associated with the formation of widespread layers exhibiting soft sediment deformation, which are interpreted to be seismite layers. The uppermost part of the Lisan section, about 5 m, is not faulted, hence the last cluster of slip events ended about 25 ky ago. The clusters of activity of individual faults coalesce to form larger clusters. These are evident in the distribution of seismite layers throughout the entire Lisan section which shows earthquake clustering during periods of ~10 ky. The clusters are separated by relatively quiescent periods of comparable duration.

Keywords: Earthquakes; Paleoseismology; Dead Sea Fault; Quaternary

1. Introduction

The present study addresses the issue of temporal distribution of surface breaking (commonly $M>6$) earthquakes on individual fault strands within a fault zone. We employ sub-centimeter stratigraphy as well as conventional paleoseismic practices to study natural outcrops of Late Pleistocene lacustrine laminites in the Dead Sea Basin near Masada. The Masada Fault Zone offers a unique opportunity to examine the rupture history of faults. We examine the number of rupture events sustained by individual fault strands, the temporal distribution of earthquakes associated with a fault zone, and the longevity of faults. The tectonic context of the study is the Dead Sea Transform fault (DST).

* Corresponding author. Tel.: +972 3 6407379; fax: +972 3 6409282.
E-mail addresses: shmulik@terra.tau.ac.il (S. Marco), amotz@cc.huji.ac.il (A. Agnon).

0040-1951/$ - see front matter © 2005 Elsevier B.V. All rights reserved.
doi:10.1016/j.tecto.2005.05.036

1.1. Late Quaternary earthquakes in the Dead Sea Basin

The Dead Sea Basin is a pull-apart graben enclosed between two overlapping segments of the Dead Sea Transform fault (Fig. 1), the boundary between the Arabian plate and the Sinai plate (Freund et al., 1968; Garfunkel, 1981; Quennell, 1956). The Dead Sea Fault is seismically active. Three sources provide information on past earthquakes: Instrumental data that have been amassed since the early 20th century, historical and archeological data that cover the last few millennia, and paleoseismic geological data that span tens of thousands of years. Reches and Hoexter (1981) and Gerson et al. (1993) initiated the paleoseismic studies along the DSF. Subsequent studies have augmented our knowledge on the seismic activity of the DSF, although many questions still await further research.

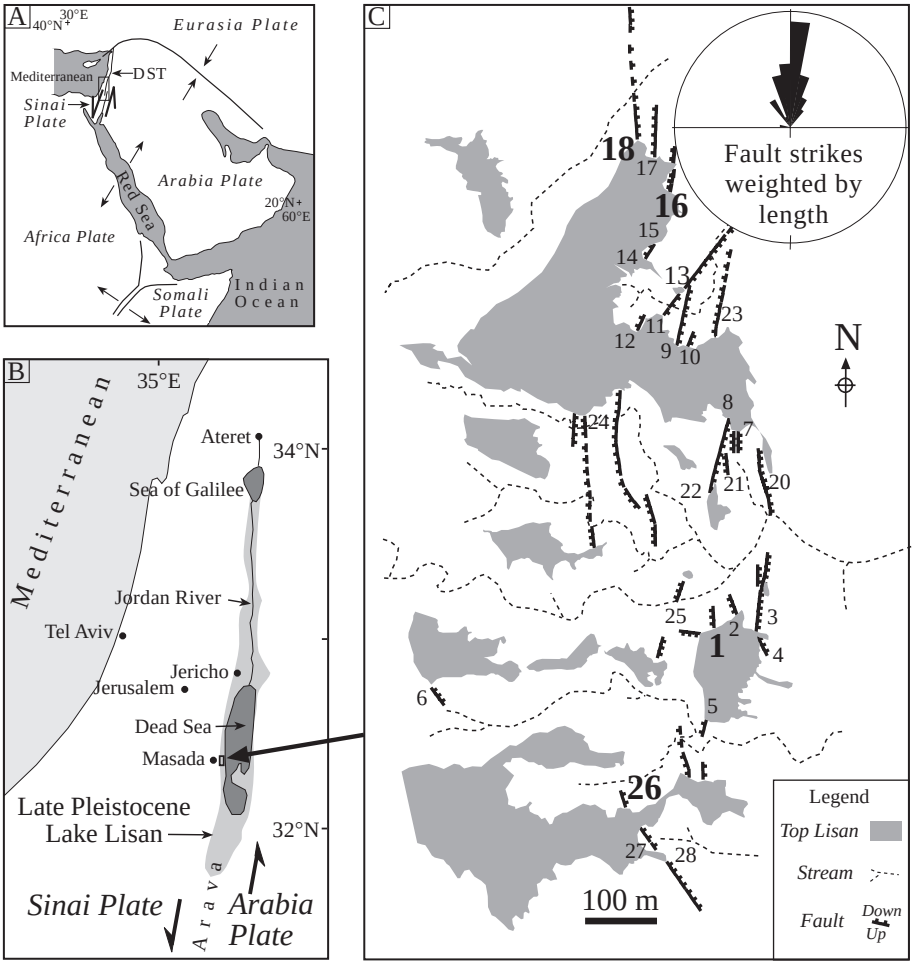

Fig. 1. (A) Tectonic plates in the Middle East. The Dead Sea Transform (DST) transfers the opening at the Red Sea to the East Anatolian Fault and the Taurus–Zagros collision zone. (B) Maximum extent of Late Quaternary Lake Lisan at 26 ka (data from Hall, 1994). (C) Map of the syndepositional fault zone near Masada. The general north–south trend parallels the Dead Sea Transform in the area and principal morphotectonic features to east and west of fault zone. The faults are all normal with planes striking north, and a few strike northeast or southeast. Dips are between 40° and 70° eastward as well as westward. Rose diagram shows strike distribution weighted by exposed fault length, largest petal is 28%. Numbers indicate documented fault exposures.

1.1.1. Geological paleoseismic records

Paleoseismic data can be acquired by recording the activity of individual faults ("on-fault studies") or fault segments and by "off-fault studies" in which the occurrence of *seismites*, layers that exhibit earthquake-triggered deformation, are documented. Marco and Agnon (1995) interpreted breccia layers, i.e., broken and mixed lacustrine seasonal laminae of the Lisan Formation in the Dead Sea Basin as seismites (Fig. 2). Marco and Agnon (1995) called them "mixed layers", a term that may cause confusion with a number of unrelated uses in the Earth sciences. We prefer to use "breccia" because it is an accurate descriptive term. Undisturbed laminated layers between these breccia layers represent interseismic intervals. The breccia layers in the lacustrine Late Pleistocene Lisan Formation and Holocene Dead Sea sediments comprise an almost continuous 70,000-year paleoseismic record in the Dead Sea Basin (Ken-Tor et al., 2001; Marco et al., 1996). A remarkable agreement between breccia-layer ages and historical earthquakes in the last 2 millennia in the DS basin supports the interpretation of the breccia layer as seismites. Evidence of combined faulting and shaking effects were recovered in the Darga alluvial fan, northern Dead Sea (Enzel et al., 2000). Paleoseismic on-fault studies revealed slip histories on marginal normal faults of the southern Arava (Amit et al., 1999, 2002; Porat et al., 1996) and the Hula basin (Zilberman et al., 2000). Strike-slip movements have been measured and dated along the Jordan Gorge Fault, north of the Sea of Galilee, where 2.2 m and 0.5 m sinistral slip occurred in the earthquakes of 1202 and 1759 respectively (Ellenblum et al., 1998). A 15-m displacement of a 5 ka stream channel gives a minimum average rate of 3 mm/year (Marco et al., 2005). Dating of offset channel deposits in alluvial fans in the northern Arava (Klinger et al., 2000; Niemi et al., 2001) yields an average Late Quaternary slip rate of about 4–5 mm/year.

1.1.2. Historical and archeological earthquake record

The people who inhabited the Middle East were aware of earthquakes. Some of their settlements have been affected by earthquakes and the remains of damage together with historical accounts, provide us with a unique record of past seismic activity in the region (e.g., Amiran et al., 1994). Archaeology can usually corroborate history although interpreting damage to ancient structures is not trivial. Damage related to earthquake shaking is recognized in numerous ruins but finding evidence for historical earthquake ruptures is extremely rare. The first such evidence from the DSF has been recovered Jericho area (Reches and Hoexter, 1981). Precise stratigraphic constraints on the age of faulting were found in the Crusader fortress of *Vadum Iacob*, now called *Ateret* (Ellenblum et al., 1998; Marco et al., 1997). The

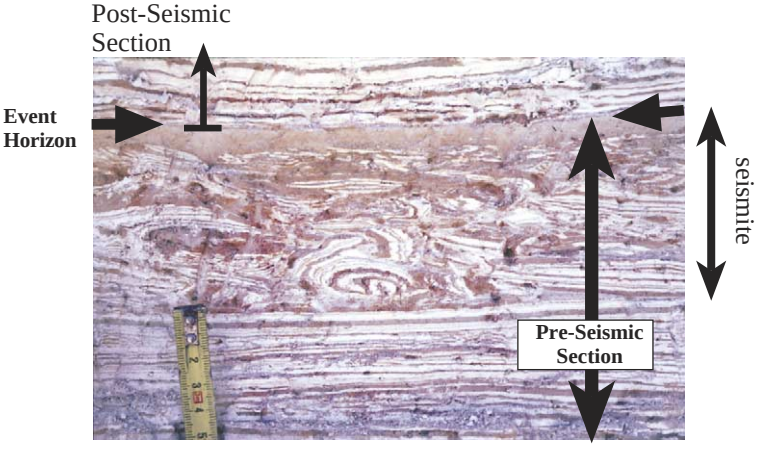

Fig. 2. Photograph of a 7-cm-thick breccia layer in the Lisan Formation showing large fragments of former laminas at the bottom and upward decrease of fragment size. The top of the breccia layer is made of pulverized laminae. We interpreted such layers as seismites, which have been formed by fluidization of upper part of the sediment at the bottom of the lake during strong earthquake shaking (Marco and Agnon, 1995).

fortress, which was built on the active trace of the fault, was torn apart twice, first by the earthquake of 1202 and again by the earthquake of 1759, in agreement with the paleoseismic observations mentioned above. A water reservoir at the Roman–Early Byzantine site Kasr-e-Tilah in the northern Arava was also offset by the fault (Klinger et al., 2000; Niemi et al., 2001).

1.1.3. Instrumental record

The seismological division of the Geophysical Institute of Israel operates the Israel Seismic Network with some 100 monitoring systems. The accrued data reveal several important characteristics. Activity is clustered in both time and in space. Since the early 1980s the most active area has been the Gulf of Aqaba, where thousands of small earthquakes cluster during periods of several months to a few years in different regions of the gulf. The activity culminated in the 22 Nov. 1995 Mw7.1 earthquake (Baer et al., 1999; Klinger et al., 1999). Most of the hypocenters are between 5 and 20 km. Focal plane solutions of other events confirm the primary sinistral motion predicted by local geology and plate tectonic considerations. Normal faulting manifests local complications in the form of stepovers. Reverse fault solutions are rare (Salamon et al., 1996; van-Eck and Hofstetter, 1989, 1990). The earthquakes largely obey the Gutenberg–Richter magnitude–frequency distribution with typical b values of 0.85–1.0 (Shapira and Shamir, 1994; Salamon et al., 1996).

1.1.4. Patterns of seismicity

By combining several disciplines including history, archaeology, and seismology, several spatio-temporal patterns begin to emerge from the data. Clustering, periodicity, and triggering have been reported in several studies. In accordance with theoretical and experimental results (e.g., Lyakhovsky et al., 2001), a temporal pattern in a century time window may resemble that of the 10,000-year window. The longest continuous off-fault record (~70–20 ka) from the Lisan Formation shows that strong ($M>6$) earthquakes cluster during periods of ~10 ky, with more quiet periods between the clusters. During the long cluster periods earthquakes appear in secondary clusters (Marco et al., 1996). A pattern of clustering is also evident in the record of the last 2 millennia in the Dead Sea (Ken-Tor et al., 2001) and in the $M>4$ record of the 20th century (Marco et al., 2001).

1.2. The Masada fault zone (MFZ)

The MFZ is a north-striking syndepositional fault zone in the western coast of the Dead Sea, near Masada, the 2000-year-old Jewish rebels' stronghold

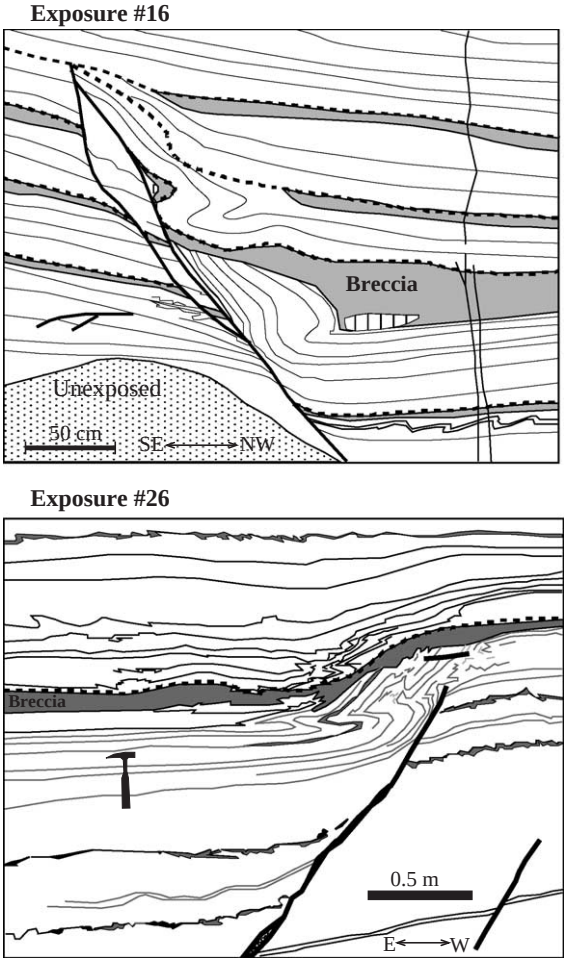

Fig. 3. Typical syndepositional fault exposures #16, #18 and #26 (see locations in Fig. 1). Line drawings are traced from photographs, emphasizing bedding, breccia layers (gray), and fault planes (solid lines). The association of faults and breccia layers indicates that the latter formed when slip occurred on the fault. Dashed thick lines are traces of the surfaces immediately after slip events, i.e., event horizons. One of the breccia layers in exposure 16 contains an embedded intraclast with vertical laminae. It probably fell from the adjacent fault scarp.

(Fig. 1). The faults, which are exposed in the Lisan Formation, were mapped in a previous study (Marco and Agnon, 1995). Most of the fault planes strike north, paralleling the main graben faults and morphological trends. The offset layers are overlain by continuous horizontal layers, indicating that the faults are syndepositional. Fault planes dip between 50° and 70° eastward as well as westward, with normal displacements up to 2 m. The average strike is $360 \pm 3.4^{\circ}$ (weighted by exposed length) with distribution pattern resembling the active graben faults. Gouges, consisting of fine aragonite and detritus breccia, calcite and some gypsum, are limited to narrow zones, commonly about 1 cm but in places up to 10 cm. Reclining folds in the hanging walls commonly accompany the faults (Fig. 3). These folds recline away from the fault planes, with horizontal axes paralleling the fault planes. Special type of layers that exhibit unusual thickness, structure, and fabric are associated with the faults in the Masada area. They are composed of massive mixtures of fine-grained matrix and tabular laminated fragments, therefore they are called 'breccia layers' (Fig. 2). Graded bedding is common where fragment-supported texture shows a gradual upward transition to a matrix-supported texture. Fragments are several millimeters to centimeters long. No imbrication, lateral grading, or other horizontal transport indicators were found. The folds are interpreted to have been formed at the top of the sediment when a fault ruptured the consolidated sediment while the footwall sediment slumped over the fault scarp and was folded. Subsequent sedimentation was followed by another fault slip that cut the fold limb (Fig. 4). Field relations show that every slip event of the faults formed a breccia layer, possibly with local slumping and folding on the fault scarp. The widespread distribution of the breccia layers also far away from the fault planes indicate that the trigger to their formation is the shaking caused by $M > 5.5$ earthquakes (a minimum for surface rupture) in the Dead Sea area (Marco and Agnon, 1995; Migowski et al., 2004).

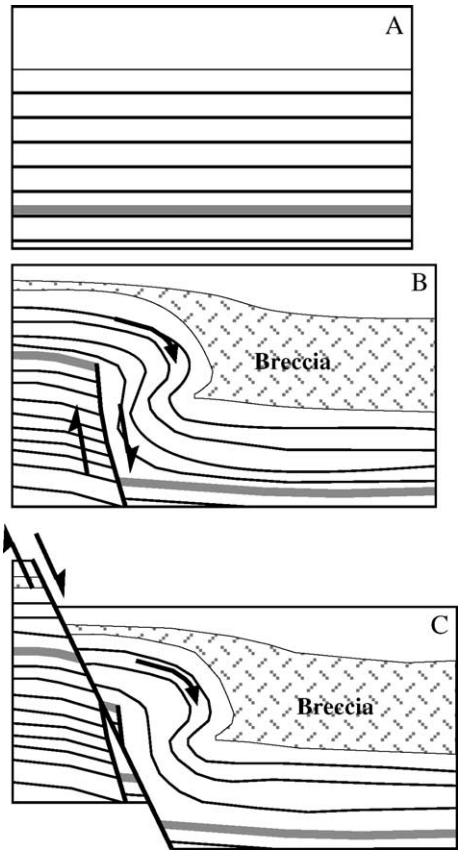

Fig. 4. A model of subaqueous faulting that explains the observed faults (Fig. 3). (A) Horizontal laminated sediment at the bottom of the lake. (B) Faulting forms a scarp (solid line) and the shaking triggers the formation of a breccia layer composed of a mixture of laminated fragments at the top of the sediment. The breccia layer is thicker in the hanging wall. Reclining folds in the hanging wall form coseismically when uppermost poorly consolidated layers slump down the fault scarp. (C) A second slip event.

2. Reconstructing slip history

We describe two detailed columnar sections on each side of several of the well-exposed N-striking normal faults in the Masada fault zone. Variations in color, aragonite/detritus proportion, and breccia layers are defined as lithostratigraphic units and used for correlation. We estimate the uncertainties in thickness of individual layers to be less than 2 cm, mainly due to lateral variation. Uncertainty in elevation may accumulate to about 5 cm.

In the example of the sections of a fault exposure (Fig. 5) we see two parts: in the lower section, up to 425 cm the stratigraphy on both sides is identical with units lying at precisely the same elevations relatively to the basal datum. The datum itself is offset 180 cm

by a normal fault, west side down. Above 425 cm the same lithological units are found on both sides but they are often thicker in the downthrown block. We interpret the thickness variation as indicator for a fault scarp at the time of their deposition. According to our model (Fig. 4B) each slip event of the fault is recog-

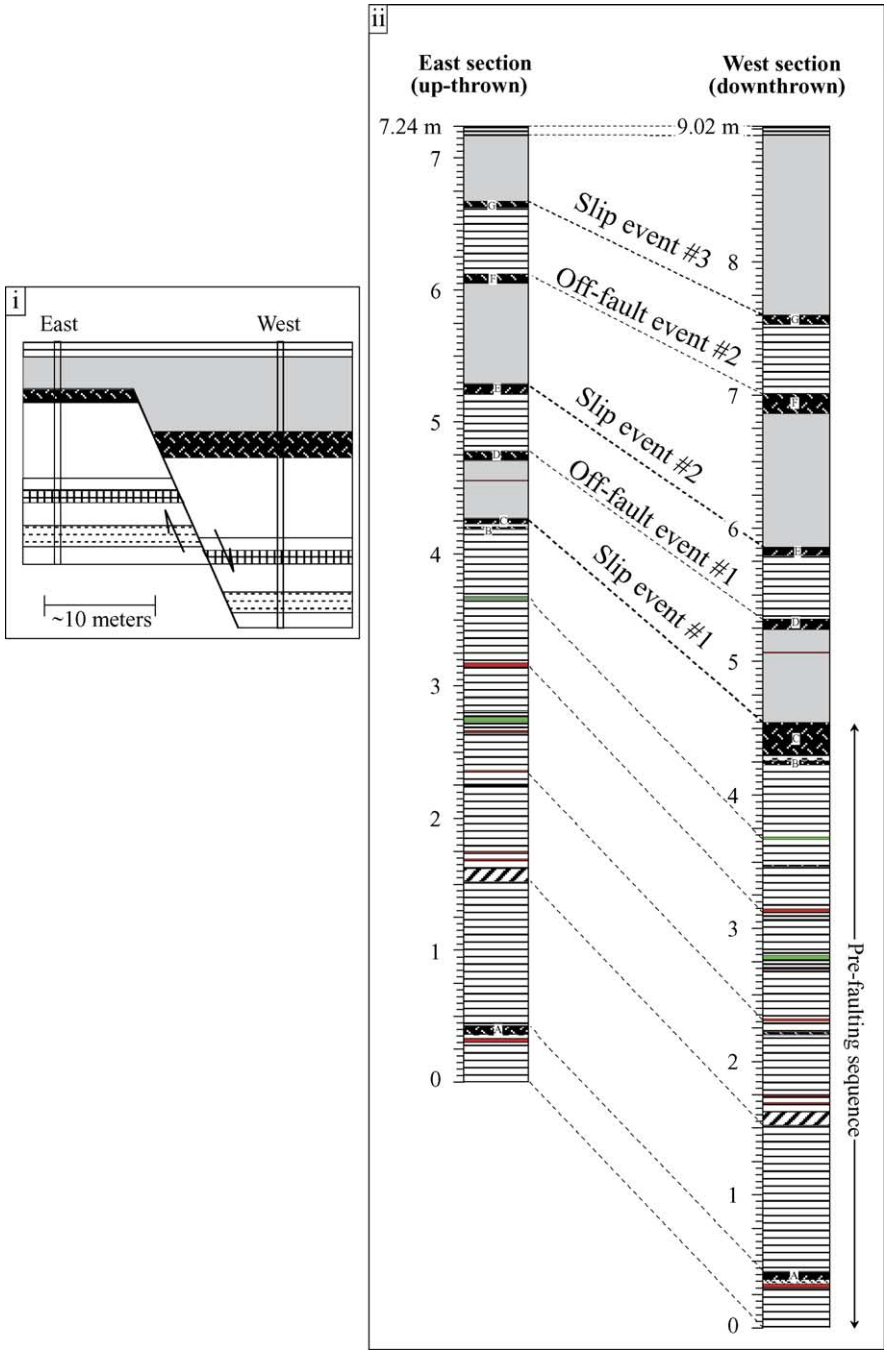

Fig. 5.

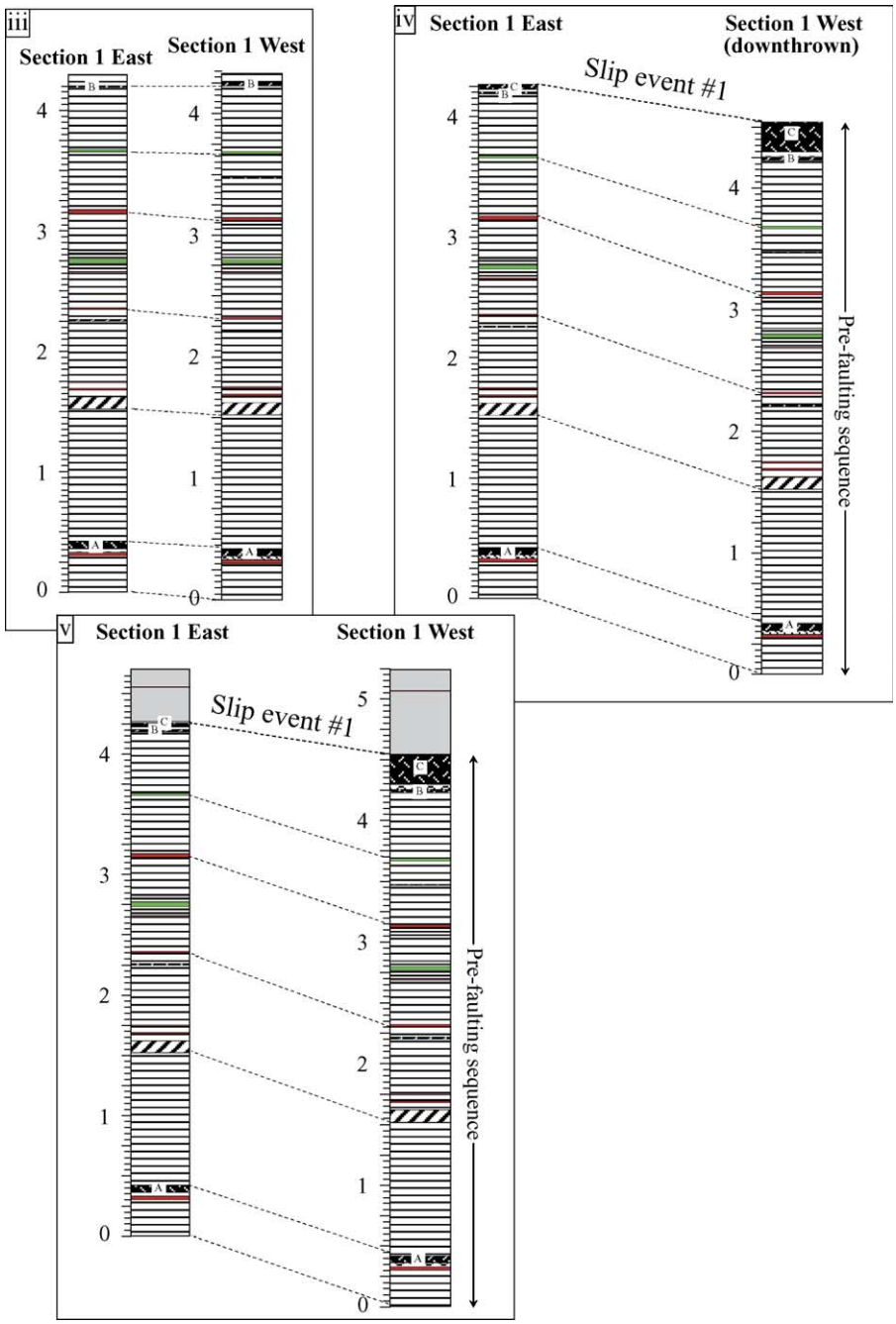

Fig. 5 (*continued*).

nized as a sequence comprising of a breccia layer at the bottom and undisturbed layers above it, which are thicker in the downthrown side. The event horizons are the tops of the breccia layers. The stratigraphy near the fault (Fig. 5) shows that the first slip event occurred after the deposition of at least 425-cm-section. This translates into 4600 years with no slip, assuming a mean deposition rate of 0.9 mm/year

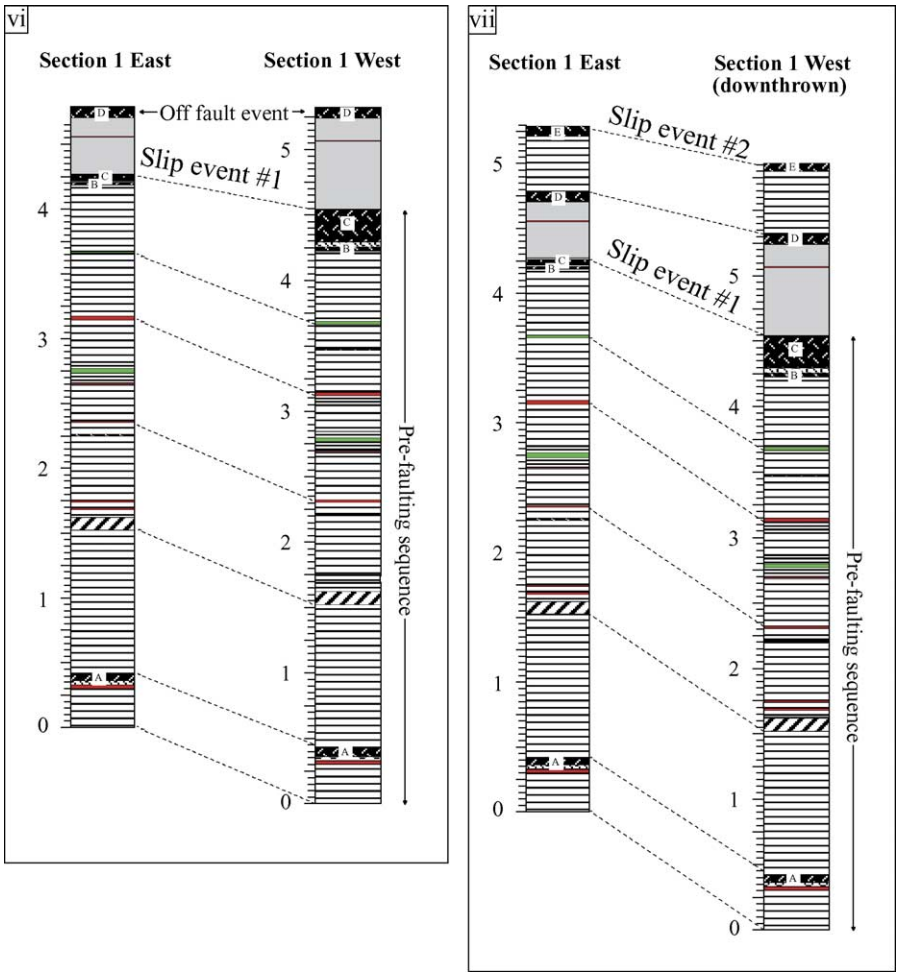

Fig. 5 (*continued*).

(Schramm et al., 2000). Subsequently, three slip events occurred within 2.4 m in the footwall or 3 m in the hanging wall, i.e., about 3000 years. Three breccia layers that are not associated with slip on this fault are also present in this part of the section. They were formed when other faults slipped. The remaining Lisan section of over 7-m above the 15-ka top of the fault, is not faulted at all, indicating altogether about 23 ky of inactivity, until the Present. Hence, the three slip events exhibit a cluster of earthquake activity, preceded and followed by quiet periods. This behavior is typical to all the faults in the MFZ. The activity of the individual faults add up to form a 10 ky long cluster of earthquakes that is apparent in the record of the breccia layers throughout the whole section (Fig. 6). None of the faults of the MFZ offset the 15 ky old top of the Lisan Formation. At present the active strand is some 3 km to the east, where a sharp break is noticed in the bathymetry of the Dead Sea (Neev and Hall, 1979), hence either the faulting activity shifted basinward or both fault zones have been active simultaneously.

3. Discussion

Temporal and spatial clustering of earthquakes can be observed in various environments, magnitude ranges, and time intervals. These include fracturing experiments, microseismicity and large earthquakes.

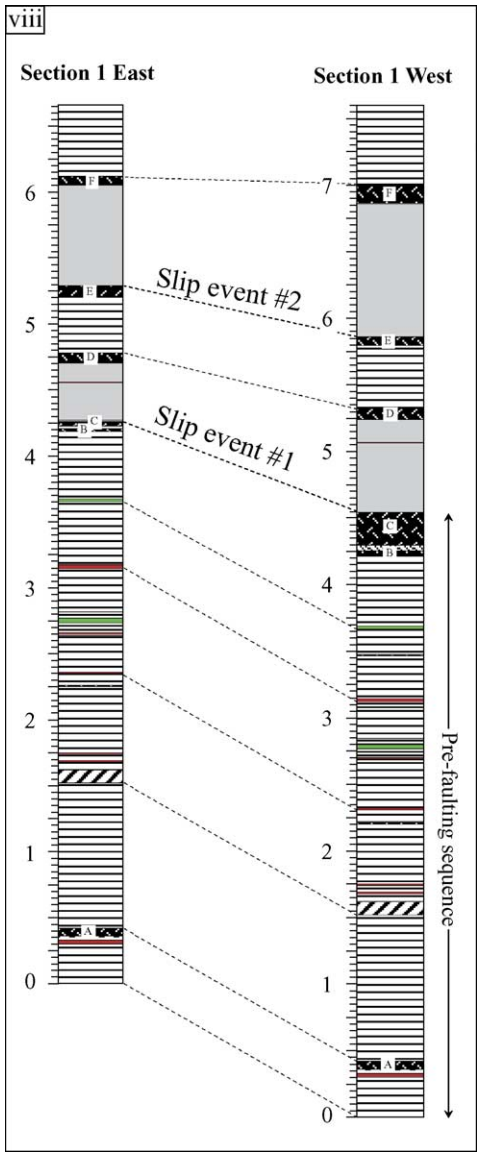

Fig. 5. Columnar sections on two sides of a syndepositional fault and step-by-step reconstruction of the sequence. (i) A schematic location diagram. The sections are about 20 m apart. (ii) Details of the observed sections on two sides of fault exposure number 1 (see location in Fig. 1). Breccia layers are named A–G (patterned-black). Datum is an arbitrary level at the base of the exposure. (iii) The lower 425 cm in the section were deposited at the bottom of Lake Lisan before the faulting began. Two earthquakes triggered the formation of breccia layer A at 40 cm and breccia layer B at 420 cm. We do not know which fault slipped concurrently with these earthquakes. (iv) When the top of the sediment was at 430 cm the first fault slip occurred. It reached the surface forming a scarp between the sections. Breccia layer C was deposited on both sides of the fresh scarp (see model in Fig. 4). Some downslope transport of material resulted with locally larger thickness of the breccia layer, up to 25 cm, in the downthrown block. (v) Sedimentation continued with a thicker section accumulating on the downthrown block until the scarp became buried (grey zones). (vi) Breccia layer D that has a constant thickness laterally is overlain by the same thickness on both sides of the fault up to breccia layer E. D is therefore interpreted as a result of an earthquake that was associated by slip on another fault. (vii) Breccia layer E, like breccia layer C, is overlain by a thicker sequence in the downthrown block, indicating a second slip on the fault. (viii) Breccia layer F is interpreted as an off-fault event because it is overlain by the same thickness up to the next breccia layer (denoted G on part i of the figure). This is the third and last slip event on this fault. The fault plane is not recognized above this level and the subsequent layers are continuous across it.

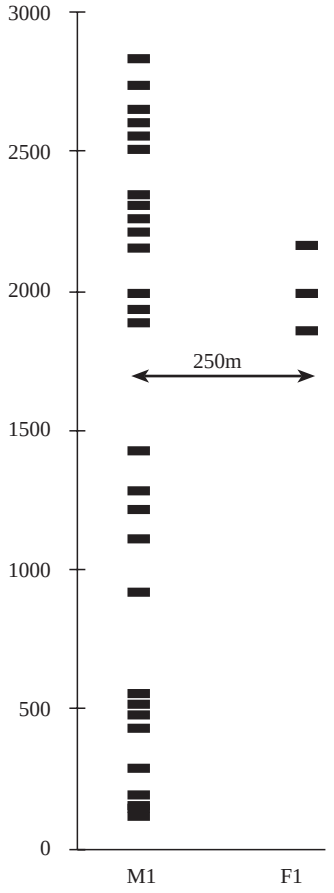

Fig. 6. The distribution of breccia layers along 28 m section of the Lisan Formation near Masada correlates with the three breccia layers that were formed during the slip events on fault #1 (Fig. 5).

Most of the data come from short-term records, <10 ky. Long-term paleoseismic records are very rare and somewhat vague, but they also indicate that earthquakes appear in clusters. For example Clifton (1968) and Dorsey et al. (1997) describe sedimentary cycles suggestive of "tectonic events" with a periodicity of tens of thousands of years, possibly related to movements on faults. Clustering is also predicted by several theoretical models (Ben-Zion and Rice, 1995; Dietrich, 1994; Lyakhovsky et al., 2001). Temporal clustering has profound effects on the viability of earthquake prediction.

Our results show a 3-ky-long cluster of up to five slip events on individual faults. These events are a part of a 10-ky-long cluster that was recorded off-fault (Marco et al., 1996). The clusters of the individual faults in the fault zone thus coalesced into a larger cluster (Fig. 6).

Several possible processes that can cause temporal clustering have been proposed.

Crack fusion: Newman and Knopoff (1983) proposed a model in which the fusion of small cracks into large ones, combined with tectonic stress release and time delays, produces repetitive clusters. The model envisions the continuous formation of a small crack population at the plate boundary due to plate driving forces. The protracted fusion of cracks results with time delay between the productions of distributed small cracks (inter-cluster periods) and the large-scale fault rupture, possibly a cluster of earthquakes.

Lyakhovsky et al. (2001) have used a distributed damage model to simulate seismicity and fault evolution. They find that recurrence may show either quasi periodicity or clustering, depending on the rate of crack healing relative to the rate of loading.

Cyclic pore pressure: A model of episodic pore pressure buildup and release (Nur and Walder, 1992) suggests a cycle duration on the order of 10^3–10^5 years. Pressure buildup followed by hydrofracturing may cause protracted stress release in the form of a cluster of earthquakes.

Episodic action of plate-driving forces: A possible mechanism of generating clusters may relate to ridge-push cycles of magma generation, injection, and reservoir replenishment.

In the southern half of the San Andreas system, migration of historical earthquakes was explained to result from creep waves induced by episodic magma injections at the East Pacific rise (King, 1987; Savage, 1971). Likewise, processes in converging plate boundaries can give rise to pulses that would be expressed in the conjugate transforms.

Alternating periods of activity between the two boundaries of the Arabian plate is observed in the historical catalogues on a century time scale. Ambraseys (1978) noted that the seismicity alternates between the North Anatolian Fault Zone and the East Anatolian Fault Zone, and that the seismic activity along the latter alternates with the DST but with longer periods of overlapping. We believe that this might be a mechanically efficient way of plate translation on longer time scales as well. During each period in the cycle a different transform is active while the other one stores the elastic energy.

4. Conclusions

Our study of individual faults within the Masada Fault Zone shows that each fault was active during a few thousands of years in which 3–5 slip events occurred on the same fault plane.

Unfaulted 20–25 ka layers of lacustrine sediments overlie the entire fault zone, indicating that it has become inactive. The active trace of the transform is at least some 3 km further east, where a sharp break in the slope of the Dead Sea margin is evident in bathymetric maps (Garfunkel et al., 1981; Neev and Hall, 1979).

The studied normal faults are secondary to the major sinistral Dead Sea Fault, but judged by the associated surface slip, they were able to generate *M*5.5–6 earthquakes.

While active, the fault zone showed clustered activity. This is evident in the distribution of seismite layers throughout the entire Lisan section which shows clustering during periods of ~10 ky separated by relatively quiescent periods of comparable duration (Marco et al., 1996). A few possible mechanisms that cause clustered activity are mentioned here but the present level of knowledge is insufficient for telling which (if any) acts in the DST.

Acknowledgments

We thank Revital Ken-Tor for her assistance in fieldwork. Constructive reviews by Anna Maria Blumetti, an anonymous referee, and the co-editors Franck Audemard and Alessandro Michetti significantly improved the manuscript. The study was funded by the Israel Science Foundation Grant 694/95 to A. Agnon and the Binational U.S–Israel Science Foundation Grant 97-286 to S. Marco.

References

Ambraseys, N.N., 1978. Studies in historical seismicity and tectonics. In: Brice, W.C. (Ed.), The Environmental History of the Near and Middle East Since the Last Ice Age. Academic Press, London, pp. 185–210.

Amiran, D.H.K., Arieh, E., Turcotte, T., 1994. Earthquakes in Israel and adjacent areas: macroseismic observations since 100 B.C.E. Isr. Explor. J. 44, 260–305.

Amit, R., Zilberman, E., Porat, N., Enzel, Y., 1999. Relief inversion in the Avrona Playa as evidence of large-magnitude historical earthquakes, southern Arava Valley, Dead Sea Rift. Quat. Res. 52 (1), 76–91.

Amit, R., Zilberman, E., Enzel, Y., Porat, N., 2002. Paleoseismic evidence for time dependency of seismic response on a fault system in the southern Arava valley, Dead Sea rift, Israel. Geol. Soc. Amer. Bull. 114, 192–206.

Baer, G., Sandwell, D., Williams, S., Bock, Y., Shamir, G., 1999. Coseismic deformation associated with the November 1995, Mw=7.1 Nuweiba earthquake, Gulf of Elat (Aqaba), detected by synthetic aperture radar interferometry. J. Geophys. Res. 104 (B11), 25221–25232.

Ben-Zion, Y., Rice, J.R., 1995. Slip patterns and earthquake populations along different classes of faults in elastic solids. J. Geophys. Res. 100, 12959–12983.

Clifton, E.H., 1968. Possible influence of the San Andreas fault on middle and probable late Miocene sedimentation, southern Caliente Range. In: Dickinson, W.R., Grantz, A. (Eds.), Conference on Geologic Problems of the San Andreas Fault System. Stanford University Publications in the Geological Sciences, pp. 183–190.

Dietrich, J., 1994. A constitutive law for rate of earthquake production and its application to earthquake clustering. J. Geophys. Res. 99, 2601–2618.

Dorsey, R.J., Umhoefer, P.J., Falk, P.D., 1997. Earthquake clustering inferred from Pliocene Gilbert-type fan deltas in the Loreto basin, Baja California Sur, Mexico. Geology 25, 679–682.

Ellenblum, R., Marco, S., Agnon, A., Rockwell, T., Boas, A., 1998. Crusader castle torn apart by earthquake at dawn, 20 May 1202. Geology 26 (4), 303–306.

Enzel, Y., Kadan, G., Eyal, Y., 2000. Holocene earthquakes inferred from a fan-delta sequence in the Dead Sea graben. Quat. Res. 53 (1), 34–48.

Freund, R., Zak, I., Garfunkel, Z., 1968. Age and rate of the sinistral movement along the Dead Sea Rift. Nature 220, 253–255.

Garfunkel, Z., 1981. Internal structure of the Dead Sea leaky transform (rift) in relation to plate kinematics. Tectonophysics 80, 81–108.

Garfunkel, Z., Zak, I., Freund, R., 1981. Active faulting in the Dead Sea rift. Tectonophysics 80, 1–26.

Gerson, R., Grossman, S., Amit, R., Greenbaum, N., 1993. Indicators of faulting events and periods of quiescence in desert alluvial fans. Earth Surf. Processes Landf. 18, 181–202.

Hall, J.K., 1994. Digital shaded-relief map of Israel and environs 1:500,000. Isr. Geol. Surv.

Ken-Tor, R., Agnon, A., Enzel, Y., Marco, S., Negendank, J.F.W., Stein, M., 2001. High-resolution geological record of historic earthquakes in the Dead Sea Basin. J. Geophys. Res. 106 (B2), 2221–2234.

King, C.Y., 1987. Migration of historical earthquakes in California. EOS Trans. 68, 1369.

Klinger, Y., Rivera, L., Haessler, H., Maurin, J.C., 1999. Active faulting in the Gulf of Aqaba: new knowledge from the Mw7.3 earthquake of 22 November 1995. Bull. Seismol. Soc. Am. 89 (4), 1025–1036.

Klinger, Y., Avouac, J.P., Abou-Karaki, N., Dorbath, L., Bourles, D., Reyss, J.L., 2000. Slip rate on the Dead Sea Transform fault in northern Araba Valley (Jordan). Geophys. J. Int. 142, 755–768.

Lyakhovsky, V., Ben-Zion, Y., Agnon, A., 2001. Fault evolution and seismicity patterns in a rheologically layered halfspace. J. Geophys. Res. 106 (3), 4103–4120.

Marco, S., Agnon, A., 1995. Prehistoric earthquake deformations near Masada, Dead Sea graben. Geology 23 (8), 695–698.

Marco, S., Stein, M., Agnon, A., Ron, H., 1996. Long term earthquake clustering: a 50,000 year paleoseismic record in the Dead Sea Graben. J. Geophys. Res. 101 (B3), 6179–6192.

Marco, S., Agnon, A., Ellenblum, R., Eidelman, A., Basson, U., Boas, A., 1997. 817-year-old walls offset sinistrally 2.1 m by the Dead Sea Transform, Israel. J. Geodyn. 24 (1–4), 11–20.

Marco, S., Agnon, A., Rockwell, T.K., 2001. Patterns of earthquake recurrence: initial results from the Dead Sea Transform. In: Litchfield, N.J. (Ed.), Ten Years of Paleoseismology in the ILP: Progress and Prospects. Institute of Geological and Nuclear Sciences Information Series, Kaikoura, New Zealand, p. 85.

Marco, S., Rockwell, T.K., Heimann, A., Frieslander, U., Agnon, A., 2005. Late Holocene slip of the Dead Sea Transform revealed in 3D palaeoseismic trenches on the Jordan Gorge segment. Earth Planet. Sci. Lett. 234, 189–205.

Migowski, C., Agnon, A., Bookman, R., Negendank, J.F.W., Stein, M., 2004. Recurrence pattern of Holocene earthquakes along the Dead Sea transform revealed by varve-counting and radiocarbon dating of lacustrine sediments. Earth Planet. Sci. Lett. 222 (1), 301–314.

Neev, D., Hall, J.K., 1979. Geophysical investigations in the Dead Sea. Sediment. Geol. 23, 209–238.

Newman, W.I., Knopoff, L., 1983. A model for repetitive cycles of large earthquakes. Geophys. Res. Lett. 10 (4), 305–308.

Niemi, T.M., Zhang, H., Atallah, M., Harrison, B.J., 2001. Late Pleistocene and Holocene slip rate of the Northern Wadi Araba fault, Dead Sea Transform, Jordan. J. Seismol. 5, 449–474.

Nur, A., Walder, J., 1992. Hydraulic Pulses in the Earth's Crust, Fault Mechanics and Transport Properties of Rocks. Academic Press, London, pp. 461–473.

Porat, N., Wintle, A.G., Amit, R., Enzel, Y., 1996. Late Quaternary earthquake chronology from luminiscence dating of colluvial and alluvial deposits of the Arava Valley, Israel. Quat. Res. 46, 107–117.

Quennell, A.M., 1956. Tectonics of the Dead Sea rift, Congreso Geologico Internacional, 20th session. Asociacion de Servicios Geologicos Africanos, Mexico, pp. 385–405.

Reches, Z., Hoexter, D.F., 1981. Holocene seismic and tectonic activity in the Dead Sea area. Tectonophysics 80, 235–254.

Salamon, A., Hofstetter, A., Garfunkel, Z., Ron, H., 1996. Seismicity of the eastern Mediterranean region: perspective from the Sinai subplate. Tectonophysics 263, 293–305.

Savage, J.C., 1971. Theory of creep waves propagating along a strike-slip fault. J. Geophys. Res. 76 (8), 1954–1966.

Schramm, A., Stein, M., Goldstein, S.L., 2000. Calibration of the ^{14}C time scale to 50 kyr by ^{234}U–^{230}Th dating of sediments from Lake Lisan (the paleo-Dead Sea). Earth Planet. Sci. Lett. 175, 27–40.

Shapira, A., Shamir, G., 1994. Seismicity Parameters of Seismogenic Zones in and around Israel. Z1/567/79(109). Institute for Petroleum Research and Geophysics.

van-Eck, T., Hofstetter, A., 1989. Microearthquake activity in the Dead Sea region. Geophys. J. Int. 99, 605–620.

van-Eck, T., Hofstetter, A., 1990. Fault geometry and spatial clustering of microearthquakes along the Dead Sea–Jordan rift fault zone. Tectonophysics 180, 15–27.

Zilberman, E., Amit, R., Heimann, A., Porat, N., 2000. Changes in Holocene paleoseismic activity in the Hula pull-apart basin, Dead Sea Rift, northern Israel. Tectonophysics 321 (2), 237–252.